**Computational Assessment of Relative Sites Stabilities and Site-Specific Adsorptive Properties of Titanium Silicalite-1**

# Computational Assessment of Relative Sites Stabilities and Site-Specific Adsorptive Properties of Titanium Silicalite-1

Matteo Signorile,[1] Alessandro Damin,[1*] Francesca Bonino,[1] Valentina Crocellà,[1] Gabriele Ricchiardi,[1] Carlo Lamberti,[1,2] and Silvia Bordiga[1]

[1] Department of Chemistry, NIS and INSTM Reference Centre, Università di Torino, Via G. Quarello 15, I-10135 and Via P. Giuria 7, I-10125, Torino, Italy

[2] International Research Center "Smart Materials", Southern Federal University, Zorge Street 5, 344090 Rostov-on-Don, Russia

**ABSTRACT:** Titanium Silicalite-1 (TS-1), because of its crystalline structure and its well-defined Ti sites, represents the prototype of a single site catalyst. According to this fundamental aspect and to the relevant role of TS-1 as selective catalyst in important industrial partial oxidation reactions, TS-1 has been widely characterized through both experimental and computational techniques. Still, several fundamental aspects of its structural and catalytic properties have to be addressed. Among these, an intriguing topic is the Ti location in the various sites of the MFI framework. The independent sites are generally considered to be 12, following the *Pnma* space group of TS-1 at high Ti loading. However, when Ti loading is lower than 2 atoms per unit cell, diffraction showed as the system must be described by the $P2_1/n$ space group, thereby allowing 24 independent sites. With respect to previous studies, this work aims to exploit this datum to give a more accurate description of the TS-1 system at low Ti loadings, adopting a state of the art methodology (all electron periodic B3LYP-D2 calculations). The relative stabilities of the 24 Ti sites have been evaluated, showing a good agreement with previous studies. The simulation of adsorption energies for ammonia (present as reactants in some of the most important industrial reactions catalyzed by TS-1) over the most stable sites have been computed as well, in order to validate the obtained models. Additionally to binding energies, adsorption enthalpies and Gibbs free energies have been obtained through an approximate reduced Hessian scheme. The improved local description of the Ti sites (in combination with the adducts stabilities given by the energetic data) allowed the deep understanding of subtle effects, such as the number of molecular ligands each Ti atom can actually host upon adsorption. These results, showing only few sites can efficiently host two ligands in the neighborhoods of STP conditions, allowed for the first time the heterogeneity in the experimental outcomes reported over the last two decades to be rationalized.

## 1. INDRODUCTION

Titanium Silicalite-1 (TS-1) is a well-known zeolite-based catalyst with MFI framework topology.[1] The peculiarity of TS-1 is represented by its active sites, *i.e.* single Ti atoms isomorphously substituting Si in the zeolitic framework. Such sites, in combination with aqueous hydrogen peroxide, are able to catalyze a variety of partial oxidation reactions, among which olefins epoxidation and cyclohexanone ammoximation are the most relevant and presently industrially exploited.[2–9] The low loading of Ti which can be inserted (below 3 $_{wt}$% of $TiO_2$) and the high dispersion of the substituent atoms across the framework positions make TS-1 a potential example of single site catalyst, *i.e.* a material where all the active sites have (in first approximation) a similar local structure and catalyze the same reaction through the same mechanism. In this regard, TS-1 represents an optimal material for fundamental research, both with experimental or computational approaches. A large number of experimental works dealing with TS-1 is available,[10–27] whereas the fraction of theoretical papers is significantly lower.[28–35] Among the latter, even less modeled TS-1 as a periodic system.[28,30,32,33] The reasons are most probably the size of the structure (288 independent atoms if $P_1$ symmetry is considered, as in a single Ti substitution per unit cell) and the flexibility of the MFI framework intrinsically connected to the wide range of bond angles and energies which Si-O-Si angle can span.[36–39] The former drawback has been progressively overcome, following the evolution of both computational resources and codes. Instead, the latter remains an intrinsic problem of the MFI topology, which must be necessarily addressed. Even if some properties can be simulated through model systems (*e.g.* Ti chabazite,[34,40–42] where Ti was inserted in the highly symmetric CHA framework[43]) the explicit modeling of the MFI topology is compulsory in order to observe peculiar effects related to TS-1. As an example, an open question relates to the capability of the various Ti sites to adsorb ammonia, a point that is relevant in some important reactions catalized by TS-1 such as cyclohexanone ammoximation.[2–4] Pioneering studies combining extended X-ray absorption fine structure (EXAFS) and calorimetric data showed as the adsorption of two $NH_3$ molecules per site is possible,[44,45] whereas more recent studies performed with valence to core X-ray emission spectroscopy (vtc-XES) lean toward a single molecule adsorption.[46] A weak point of the previous approaches is the average picture over all the Ti sites that these techniques offer on. In this regard, a proper simulation can helpfully drive the experiment interpretation. MFI models have to be exploited, indeed the adsorptive properties are most probably determined by local effects (such as the positioning of Ti sites with respect to the zeolitic framework). According to the last point, each possible substitution of Si with Ti generating an

independent site must be taken into account. Previous works always referred to TS-1 as derived from the orthorhombic (*Pnma* space group) polymorph of Silicalite-1,[12,28,30,32,33] but already its discoverers reported as it belongs to the $P2_1/n$ monoclinic space group when the Ti loading is < 2 atoms/cell,[10] or at cryogenic temperatures: Marra *et al*.[47] have shown that an activated TS-1 sample (2.6 wt.% in $TiO_2$) undergoes a *Pnma* to $P2_1/n$ at 170 K. Thereby, since Ti sites are considered separately through single substitutions, this study considered the monoclinic Silicalite-1 (S1) as the correct starting point for simulation. This implies also that the number of independent Ti sites is doubled (from 12 to 24), increasing the number of structures to be considered. The 24 structures have been relaxed and ranked on the basis of their relative stabilities: two different computational strategies were adopted and, for each site, the lowest achieved energy was coherently chosen as the "most correct one". Such procedure allowed selecting the most probable substitutions, *i.e.* the most abundant Ti sites. Finally, a detailed study of $NH_3$ adsorption over the most stable sites has been performed. In detail, the focus has been put on the adsorption capability of these sites, in terms of number of $NH_3$ molecules which can be adsorbed. The aim is to shed light on this debated property of TS-1 through a critically comparison with experimental results.

## 2.COMPUTATIONAL DETAILS

TS-1 models were constructed starting from a siliceous Silicalite-1 structure, derived by Artioli and coworkers by neutron diffraction.[48] As previously discussed, the model has $P2_1/n$ symmetry, in agreement with experimental findings from TS-1 discoverers.[10] In Figure 1, the position of the 24 independent T sites within the MFI unit cell is highlighted.

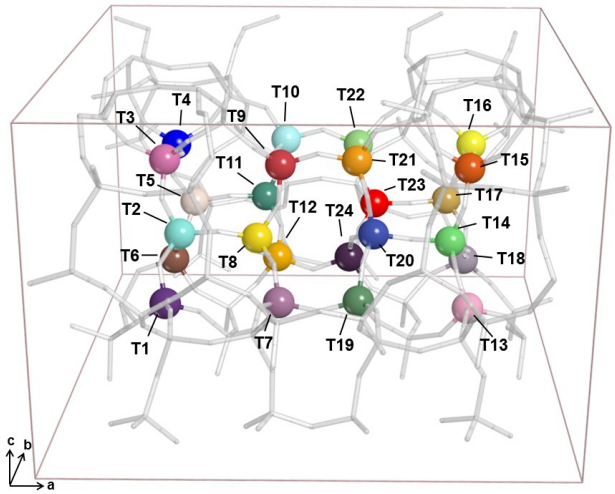


Figure 1. Pictorial representation of the 24 independent T sites within the MFI unit cell (having $P2_1/n$ symmetry). Colors are arbitrary chosen for sake of visualization.

In order to compare the results from this paper with the previous literature (dealing with TS-1 described as orthorhombic), it is useful to exploit the following relation:

$$T_M = T_O + n \cdot 12 \ , \ n = 0{,}1 \qquad (1)$$

where $T_M$ is the label of an independent Ti sites in the monoclinic structure (ranging fro 1 to 24), $T_O$ is the label of an independent Ti sites in the orthorhombic structure (ranging fro 1 to 12) and $n$ is an integer which can assume 0 or 1 as values. Where not specified, the label "T" hereafter always refers to the monoclinic sites ($T_M$).

Two different computational approaches were followed: in the first one, the Silicalite-1 structure was pre-optimized exploiting the CRYSTAL14 code,[49] with the B3LYP-D2 functional (*i.e.* combining the B3 hybrid exchange functional[50] with the LYP correlation functional[51] and including empirically dispersive forces according to the Grimme D2 scheme[52]). As demonstrated in our previous study on Ti-CHA,[42] dispersive forces are of outmost importance in the correct description of the adsorption of molecules over the Ti sites, thus were systematically included in the calculations. Then, Ti substitution was performed and the derived TS-1 structures relaxed (again through the B3LYP-D2 method). In the following, this method will be referred to as "B3LYP-D2 only". In the second approach, a preliminary Molecular Mechanics (MM) relaxation through the GULP code[53] was initially adopted, exploiting the Force Field (FF) proposed by Sierka and Sauer for the siliceous framework,[54] whereas parameters for Ti from Ricchiardi and Sauer were considered.[28] Structures obtained from MM were further optimized within the CRYSTAL14 code, through a periodic B3LYP-D2 approach. This last scheme will be hereafter labeled as "FF → B3LYP-D2". Such approach enabled (through the FF pre-optimization) the generation of new structures to be exploited as initial guess for the consequent high-level calculations, thus potentially allowing different portions of the Potential Energy Surface (PES) inaccessible by bare B3LYP-D2 to be explored.

The same basis set and computational parameters recently exploited in our study on Ti chabazite (Ti-CHA) were employed in this study.[42] In detail, titanium, silicon and oxygen atoms were described through a 86-411G(d31),[55] 88-31G(d1),[56] and 8-411G(d1)[56] basis respectively. In ammonia adsorption simulations, nitrogen and hydrogen atoms were respectively described with a TZV2P and a TZV basis set from Ahlrichs.[57] The truncations for the mono- and bi-electronic integral (TOLINTEG) were set to {777714}. The sampling in the reciprocal space (SHRINK) was set to {2 2}, for a total of 8 *k* points. The maximum order of shell multipoles

in the long-range zone for the electron-electron Coulomb interaction (POLEORDR keyword) was chosen to be 6. All the other parameters were set to default values according to the CRYSTAL14 manual.[58]

Such calculation was repeated over the 24 independent crystallographic sites of the monoclinic MFI framework and the resulting TS-1 structures were ranked in terms of relative stability. The two rankings built through the B3LYP-D2 only and the FF → B3LYP-D2 approaches were compared in terms of absolute energies, thus generating a third ranking where the lowest energy for each T site was selected.

Reaction energies for the $Si \rightarrow Ti$ substitution were computed as well, in order to allow a direct comparison with previous literature.[30,40] In detail, the reaction hereafter reported was considered:

$$S1 + TiO_2(rutile) \rightarrow TS1 + SiO_2(\alpha - quartz) \quad (2)$$

Reaction energies $\Delta E_{sub}$ were consequently computed as:

$$\Delta E_{sub} = E(TS1) - E(S1) + E(SiO_2) - E(TiO_2) \quad (3)$$

Such hypothetical solid-state reaction was preferred to other proposed in the literature (*e.g.* see Ref. [28,33]) to better suit the periodic computational approach adopted in this work, indeed giving better results with solid systems.

Ammonia adsorption was then simulated over the three most stable sites, according to the following general reactions:

$$TS1 + NH_{3,gas} \rightarrow (TS1 + NH_3)_{adduct} \quad (4)$$

$$(TS1 + NH_3)_{adduct} + NH_{3,gas} \rightarrow (TS1 + 2NH_3)_{adduct} \quad (5)$$

The Binding Energies for the two processes were then computed according to Equations 6 and 7:

$$BE^1 = E(TS1) + E\left(NH_{3,gas}\right) - E((TS1 + NH_3)_{adduct}) \quad (6)$$

$$BE^2 = E((TS1 + NH_3)_{adduct}) + E\left(NH_{3,gas}\right) - E((TS1 + 2NH_3)_{adduct}) \quad (7)$$

where $E(TS1)$ is the energy of the bare TS-1, $E\left(NH_{3,gas}\right)$ is the energy for isolated $NH_3$ and $E((TS1 + NH_3)_{adduct})$ and $E((TS1 + 2NH_3)_{adduct})$ represent the energies for the single and double TS-1–$NH_3$ adducts respectively. These binding energies were BSSE corrected according to the counterpoise method,[31] thereby according to Equation 8:

$$BE^c = BE - [E_a(A^{def}) - E_{ab}(A^{def}) + E_b(B^{def}) - E_{ab}(B^{def})] \quad (8)$$

The correction is achieved subtracting from the bare BE a term related to the energies of the adduct monomers (here labeled as "A" and "B") after these have been geometry relaxed upon adsorption (as pointed out by the "$^{def}$" superscript). Their energies have been computed considered their only basis functions ("$_a$" and "$_b$" subscripts) or including the functions for the other monomer as well ("$_{ab}$" subscript). From the definition of $BE^c$ given in Equation 8, recasted considering explicitly the BE term, the interaction can be split in two contributions as reported hereafter:

$$BE^c = E_a(A) + E_b(B) - E_{ab}(AB) - [E_a(A^{def}) - E_{ab}(A^{def}) + E_b(B^{def}) - E_{ab}(B^{def})] \quad (9)$$

$$BE^c = [E_{ab}(A^{def}) + E_{ab}(B^{def}) - E_{ab}(AB)] + [E_a(A) - E_a(A^{def}) + E_b(B) - E_b(B^{def})] \quad (10)$$

$$BE^c = BE^{c\,int} + DE \quad (11)$$

The two terms of Equation 11 (DE and $BE^{cint}$) takes into account the energetic cost of monomers deformation upon adsorption and the pure interaction contribution to the BE respectively.

In order to obtain a better comparison with the experimental adsorption data (which are adsorption heats), adsorption enthalpies were estimated through the calculation of vibrational frequencies. Since these can be calculated only numerically (with an unsustainable computational cost over the whole system), as first approximation a reduced Hessian was computed, including only the displacements from the $Ti(OSi)_4$ moiety and the adsorbed molecules. Adsorption Gibbs free energies were computed as well. All the calculations were carried out considering Standard Temperature and Pressure (STP) conditions, *i.e.* 298.15 K for temperature and 1 bar for pressure. The stability of $NH_3$ bi-adducts was further checked, since the capability of TS-1 to adsorb one or two ammonia molecules is debated.[42,44–46] Therefore, the Gibbs free energy was specifically computed for the desorption of the second ammonia molecule (*i.e.* the inverse of the process described by Equation 5) too, as function of temperature and pressure. Temperature and pressure ranges have been selected on the basis of the experimental conditions exploited in research work discussed together with present results.[44–46] It is worth to mention that the obtained thermochemical results (especially concerning Gibbs free energies) have been obtained in an approximate way, then only allowing a qualitative discussion with respect to experimental results. A more detailed description would require: i) the inclusion of a higher number of atoms (possibly all) in the calculation of the Hessian; ii) the exploitation of a proper formalism (*e.g.* taking into account anharmonicity effects) in the calculation of Gibbs free energies.[59]

## 3. RESULTS AND DISCUSSION

### 3.1 T SITES STABILITY

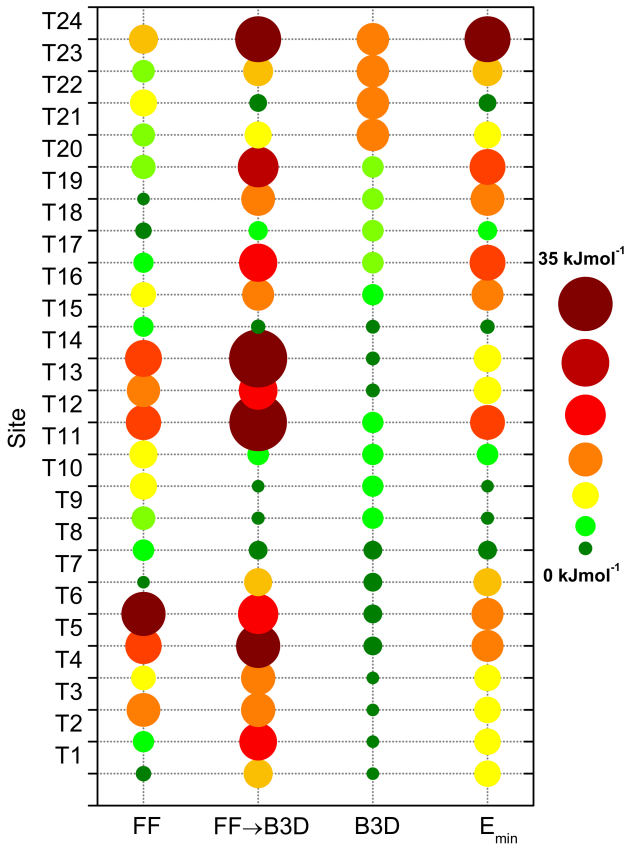


Figure 2. Relative stabilities of Ti sites placed in the 24 T sites of MFI, evaluated through: a B3LYP-D2 relaxation starting from the experimental geometry (B3D), a B3LYP-D2 relaxation starting from a geometry previously relaxed through FF (FF→B3D) and a combined ranking obtained by choosing the lowest absolute energy from the previous calculations for each site (Emin). The ranking obtained from the only FF relaxation (FF) is reported for completeness. On the right, the quantification of the used symbols is reported from 0 (green) to 35 kJmol−1 (brown), by step of 5 kJmol−1.

Figure 2 shows the relative stability of the 24 possible Ti sites of a single-substituted TS-1. The numerical values for such relative stabilities are listed in Table S1 of the Supplementary Content. A clear difference among the trends obtained with the two different computational strategies adopted is observed. The "B3LYP-D2 only" calculations show as the sites "pack" in a limited number of subsets, namely six different families can be distinguished. Another interesting feature is represented by the low spread of the relative stability values among these subgroups: 20 sites over 24 show a relative stability lower than 10 kJmol$^{-1}$. These rather low values do not clearly depict which T sites are favored to host Ti. For this reason, the second calculation strategy (FF → B3LYP-D2) was attempted. The pre-relaxation performed through FF allowed a different portion of the PES to be explored, bringing the model toward a totally new initial guess. Upon the consequent B3LYP-D2 optimization, a more articulated situation with a higher spreading of the relative stabilities of the various T sites, is observed. According to these calculations, the most stable sites are T9, T10 and T15, followed by the T8, T11, T18 and T22 sites. All the other sites lay in a range of stabilities ranging from 10 kJmol$^{-1}$ up to almost 40 kJmol$^{-1}$, suggesting that their occupancy is not favored. Furthermore, with respect to the bare FF ranking, the exploitation of B3LYP-D2 completely alters the sites stabilities, testifying as the adopted FF just helped to explore the PES, anyway without giving reasonable results by itself. The two rankings presented above here demonstrate as the PES associated to the TS-1 structure is rather complex and difficult to explore, since different starting points could bring to different energy minima. In this regard, even if dynamic methods represent the election tool toward this type of study, these haven't been applied in this preliminary stage since their unaffordable cost at the desired level of theory. However, in order to give the best possible description, the previous datasets were compared in terms of absolute energies (see Table S1, $E_{abs}$ columns for B3D, FF → B3D and $E_{min}$ methods) and the lowest value for each site was kept. This strategy allows selecting the best possible solution achievable within the available dataset, since the lowest energy point will correspond to the deepest minimum reachable through the computational method applied in this work. Even if the spreading of the values is reduced with respect to FF → B3LYP-D2, the various sites are still sufficiently "energetically resolved" to clearly categorize them. Again, the three most stable sites are T9, T10 and T15, with a relative stability spreading lower than 2 kJmol$^{-1}$. With respect to previous data, both experimental[12,33,47,60,61] and computational[28,30,32,33,62–65], the T10 and T15 (the latter corresponding to $T_O3$ in the *Pnma* MFI structure) are often found as the most probable sites, whereas T9 is rarely reported.

The other low energy sites (T8; T11; T18 corresponding to $T_O6$; and T22 corresponding to $T_O11$) also frequently occur in the literature.

In order to make a more direct comparison with computational literature,[30,40] absolute substitution energies were calculated according to the hypothetical reaction reported in Equation (2). The graphical outline of these results is given in Figure S1, whereas the numerical values are reported in Table S2 of the Supplementary Contents. According to the calculations, the substitution reaction is not favored in any site, with reaction electronic energies falling in the 80-110 kJmol$^{-1}$. The result is absolutely reasonable in comparison with reference literature data: Zicovich-Wilson and Dovesi reported substitution energies in the 80-105 kJmol$^{-1}$ range for Sodalite and Chabazite exploiting a periodic Hartree-Fock approach;[40] later Gale studied the substitution of Ti in the 12 independent sites of *Pnma* TS-1 with a pure DFT method (PBE), obtaining reaction energies in the 85-110 kJmol$^{-1}$.[30] The present results correctly fit in a similar energy region, testifying the reliability of the approach.

### 3.2 GEOMETRICAL FEATURES

The evaluation of the goodness of computed geometrical parameter is not trivial, since the number of structures to be compared. A direct comparison of the features derived for each of the 24 structures with experimental data could be misleading, since some of the sites are expected to be scarcely populated according to their instability. Critically considering the structural data available from experimental techniques (mainly powder X-ray and neutron diffraction and EXAFS spectroscopy), they represent an average over the whole measured sample. The adopted strategy was then to average the computational data too: two strategies were attempted, exploiting the "$E_{min}$" dataset of structures.

**Table 1. Averaged geometrical parameters for the TS-1 structures: cell parameters (*a, b, c*) and angles (α, β, γ), cell volume (V), its expansion with respect to siliceous Silicalite-1 (ΔV) and average Ti-O distance (<Ti-O>). All the lengths are given in Å, the angles in °, the volume in Å$^3$, the volume expansion in percentage.**

| Method | Ref | a | b | c | α | β | γ | V | ΔV/V[a] | <Ti-O>[b] |
|---|---|---|---|---|---|---|---|---|---|---|
| Arithmetic average | TW | 19.724 | 19.992 | 13.343 | 90.0 | 91.1 | 90.0 | 5260 | 0.42 | 1.805±0.002 |
| *k* weighted average | TW | 19.725 | 19.965 | 13.339 | 90.0 | 91.2 | 90.0 | 5252 | 0.26 | 1.806±0.004 |
| Laboratory XRPD | 10 | 19.907 | 20.108 | 13.381 | 90.0 | 90.6 | 90.0 | 5356 | 0.30 | – |
| Synchrotron XRPD | 11 | 19.911 | 20.118 | 13.399 | 90.0 | 90.3 | 90.0 | 5367 | 0.31 | – |
| Neutron PD | 12,48 | 19.907 | 20.072 | 13.385 | 90.0 | 90.0 | 90.0 | 5348 | 0.39 | – |
| Synchrotron EXAFS | 66 | – | – | – | – | – | – | – | – | 1.793±0.007 |

[a] the volume expansion is calculated with respect to the Silicalite-1 volume, *i.e.* ΔV = [V(TS-1) – V(S-1)] / V(S-1). The volume of Silicalite-1, together with its cell parameters, is given in Table S3.

[b] the uncertainness on computational data was calculated through error propagation. The standard deviation on the average of the four Ti-O distances for each TS-1 structure was took as its uncertainness.

In the first one, the simple arithmetic average of the main features (cell parameters, volume and average Ti–O distance) was taken. In the second strategy, a weighted average was performed, using as weight an indicator of the relative population of each T site. An equilibrium-constant-like parameter *k* was in first approximation then calculated applying the following well-known relation:

$$\ln k = -RT\Delta G \qquad (12)$$

Since the ΔG values are not available, $\Delta E_{sub}$ was used instead. The temperature was arbitrary set to 298.15 K. As *k* is related to the probability that substitution occurred in a given T site (*i.e.* to the concentration of such substituted site), it clearly relates to its occupancy by Ti.

In this regard, it is possible to evaluate that T10, T9 and T15 account for more than 80% of the Ti-substitued sites (32.2%, 30.2% and 17.8% respectively), whereas each other position shows occupancy lower than 10% (see Table S3, column Occ). Even if the evaluation of *k* is rather rough, it could help in giving a better average description. The results achieved through the two averaging strategies are reported in Table 1 and compared with experimental results.[10,11,66] For completeness, the whole set of geometrical parameters for each site (including the *k* weights) is reported in Table S3 and the full structures (given in fractional coordinates) are available in the Supporting Information. Upon averaging of computational parameters, both strategies give similar results. Therefore, our energy ranking is neither validated nor falsified by the experimental structural parameters. However it provides a set of representative structures which constitute a safe ground for method validation and the adsorption studies. Referring to Silicalite-1 (see Table S1), the obtained geometrical descriptors show as B3LYP-D2 underestimates the cell parameters and thus the cell volume. Referring to the experimental geometry proposed for the $P2_1/n$ Silicalite-1,[10,11,48] the computed cell parameters are 0.5-0.8% shorter than expected. Consequently, the calculated cell volume is about 2% lower of the experimental ones. A possible explanation

for such behavior is the difficult description of the floppy siloxane bridges. As reported in several benchmark studies involving simple models of the Si-O-Si moiety, its correct description in terms of both geometrical and energetic features requires to adopt post Hartree-Fock methods together with large basis sets.[36–39] DFT is in general giving a poorer geometrical description, whereas it gives reasonable energetic values.[38] Furthermore, it is worth to mention that Silicalite-1 is often a defective material, *i.e.* where some Si atoms are missing, thus generating nests of interacting silanols.[67,68] These moieties bring to the expansion of the cell (since they are bulkier than a usual tetrahedral Si site),[69] thereby a direct comparison of our Silicalite-1 model (which is defect-free) to experimental data is not straightforward. Moving to the TS-1 models, the *b* and *c* parameters are correctly expanding as expected from experimental results,[10,11] whereas the *a* parameter is slightly decreasing. Again, all the cell parameters (thus the cell volume) are slightly underestimated with respect to the corresponding experimental values, in line with the previous findings on Silicalite-1. Another significant difference is found in the β angle, which increases with respect to the Silicalite-1 model (where the experimental data show a slight decrease). Conversely the α and γ are found to be right-angles, even if no symmetry constrains have been set during the geometry relaxation. What is however interesting is the good agreement in terms of volume expansion upon Ti insertion: this parameter is very sensitive, indeed it represented the first experimental evidence of the isomorphous substitution of Ti in the Silicalite-1 framework.[1] The *k* weighted average further gives a better description, giving a value very close to the experimental ones. Finally, accounting for Ti–O distances, these values are in line with the experimental ones, both in term of absolute value and of deviation from the average.

### 3.3 $NH_3$ ADSORPTION

Ammonia adsorption, at both single and double coverages, was simulated over the three most stable sites (*i.e.* T9, T10 and T15). The BSSE corrected Binding Energies ($BE^c$) are reported in Table 2 together with adsorption enthalpies and Gibbs free energies (ΔH and ΔG) estimated through a reduced Hessian calculation. $NH_3$ adsorption simulation has been performed over two further T sites with intermediate and poor relative stabilities (T4 and T24 respectively) to verify the possible difference occurring in adsorption at less-stable sites. In fact, high adsorption energies are often observed on high energy sites. The graphical outline of the structures of the single and double TS-1–$NH_3$ adducts are shown in Figure 3.

**Table 2. Main geometrical and energetic values for $NH_3$ adsorption (both single or double) over the three most stable Ti sites (T9, T10 and T15). Adsorption parameters over other two sites with intermediate (T4) and poor (T24) relative stabilities have been computed for comparison. Ti–N distances, counterpoise BSSE corrected Binding Energies ($BE^c$) and their deformational (DE) and purely interactive ($BE^{cint}$) components, adsorption enthalpies (ΔH) and Gibbs free energies (ΔG) are reported. ΔH and ΔG have been estimated through a reduced Hessian calculation at STP conditions (298.15 K, 1 bar). All the distances are given in Å, whereas energies are expressed in kJmol$^{-1}$.**

| Adduct | | Ti–N$^1$ | Ti–N$^2$ | BE$^c$ | DE | BE$^{cint}$ | ΔH | ΔG |
|---|---|---|---|---|---|---|---|---|
| T4 | + $NH_3$$^1$ | 2.315 | - | 84.2 | -47.0 | 131.2 | -74.6 | -28.7 |
| | + $NH_3$$^2$ | 2.347 | 2.307 | 18.8 | -88.7 | 107.4 | -7.7 | 36.0 |
| T9 | + $NH_3$$^1$ | 2.311 | - | 75.9 | -42.5 | 118.4 | -67.3 | -24.2 |
| | + $NH_3$$^2$ | 2.280 | 2.315 | 78.9 | -51.8 | 130.7 | -69.5 | -24.1 |
| T10 | + $NH_3$$^1$ | 2.302 | - | 91.5 | -47.7 | 139.2 | -82.5 | -38.0 |
| | + $NH_3$$^2$ | 2.328 | 2.359 | 34.2 | -64.8 | 98.9 | -25.4 | 17.7 |
| T15 | + $NH_3$$^1$ | 2.294 | - | 84.1 | -43.4 | 127.5 | -75.2 | -32.2 |
| | + $NH_3$$^2$ | 2.300 | 2.306 | 59.3 | -71.7 | 131.0 | -49.7 | -3.4 |
| T24 | + $NH_3$$^1$ | 2.320 | - | 72.0 | -42.8 | 114.8 | -65.9 | -19.6 |
| | + $NH_3$$^2$ | 2.312 | 2.327 | 60.6 | -71.3 | 131.9 | -48.0 | -4.4 |

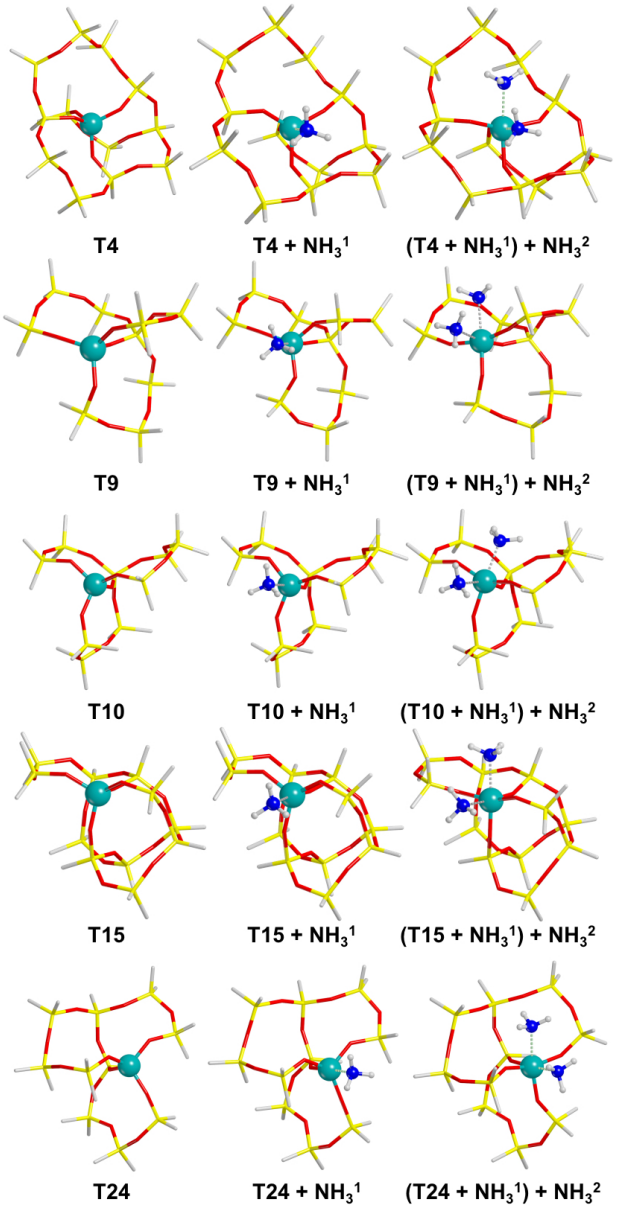


Figure 3. Structures of the single and double TS-1–NH3 adducts over the three most stable Ti sites (T9, T10 and T15). The structures for single and double TS-1–NH3 adducts over sites with intermediate (T4) and poor (T24) relative stabilities are reported for comparison.

Even possessing similar relative stabilities, the three most stable sites show remarkable differences in adsorptive properties. The T9 site presents similar $BE^c$ for both the first and the second adsorbed molecule. The same consideration stands for the estimated $\Delta H$ and $\Delta G$, both similar among the consecutive adsorptions and, most importantly, negative. As the calculations suggest, the adsorption process of ammonia over T9 site is favored for two molecules at STP conditions. A different result is achieved with T10 site, where the highly favored adsorption of the first molecule is followed by a 63% drop of the $BE^c$ upon the insertion of the second ammonia. The much lower electronic stability of the second process readily affects the other quantities, leading to a still negative (but low, in absolute terms) $\Delta H$ and to a positive $\Delta G$. The result points out that the adsorption of a second $NH_3$ molecule over the T10 site is unlikely to occur at STP conditions. Finally, T15 presents an intermediate situation: all the energetic quantities suggest that both the first and the second adsorption are possible and favored, but with a clear predominance of the first event (the $\Delta G$ value for the second adsorption event is negative but small at STP conditions). To shed light on the causes of this behavior, $BE^c$ was decomposed in its two components (*i.e.* DE and $BE^{cint}$) as defined in Eq. 9-11. Site T9 presents a slight increase of both DE and $BE^{cint}$ upon the second adsorption, finally leading to very similar $BE^c$ and justifying the conduciveness of the double adsorption process. As already expected, T10 has a totally different trend, with a second adsorption giving rise to a significant increase of DE and (mainly) to a considerable drop of $BE^{cint}$. The longest Ti-N distance, measured upon the second $NH_3$ insertion, is symptomatic of this weaker interaction. Finally, T15 pays the higher energetic price for the second $NH_3$ adsorption in terms of DE, however being compensated by the still high $BE^{cint}$ associated to the process.

The adsorptive properties of $NH_3$ over representative, less-stable sites (T4 and T24) have been computed. Site T4 shows a behavior very similar to the case of T10: the adsorption of a single $NH_3$ molecule is highly favored, whereas the insertion of the second molecule is not possible at STP conditions. Similarly, T24 mimics the adsorption occurring at site T15, with a favorable first adsorption event and a slightly favored second one. Considering interaction enthalpies, these falls in the same energetic range observed for adsorption occurring at the more stable sites, despite their higher instability logically suggest they should interact stronger with adsorbates. In this regard, the calorimetric data for $NH_3$ adsorption over TS-1 cannot be regarded as a potential method to assess Ti location in the MFI framework.

The energetic analysis of the three most stable T sites upon $NH_3$ adsorption depicts the complexity of the TS-1 system, where the local environment (as depicted in the animated structure *t9.avi, t10.avi and t15.avi,* attached as Supporting Information) around the interaction center plays major role in determining the adsorptive properties at the microscopic level. Comparing these data with the various experimental results collected over the last 20 years, it is clear that a critical interpretation of these is now feasible. An unsolved point in such discussion relates to the number of $NH_3$ molecules that a single Ti site is able to adsorb. The combined calorimetric-EXAFS results from Bolis and coworkers showed as each Ti site host 2 molecules, with heats of adsorption ranging in the 50-100 $kJmol^{-1}$ range.[44,45] Conversely, more recent results from Gallo *et al.*, obtained through vtc-XES measurements, showed as single adsorption is preferred.[46] As first comment, the calculated adsorption enthalpies reported in Table 2 correctly fit in the energetic range obtained through calorimetry studies.[44,45] Concerning the number of adsorbed molecules as derived by EXAFS or vtc-XES measurements, it is worth making some instrumental consideration on the two techniques. In both cases, intense synchrotron X-rays beams represent the excitation source, thereby exposing the sample to a continuous energy input, particularly relevant in the vtc-XES experiment performed at ESRF ID26, that used two independent undulators as photon source. The exposure time then turns to be a critical parameter: the longer the exposure, the higher the energy transferred (few to several hours are were needed to collect, with sufficient statistic, EXAFS[44,45] and vtc-XES[46] spectra, respectively).

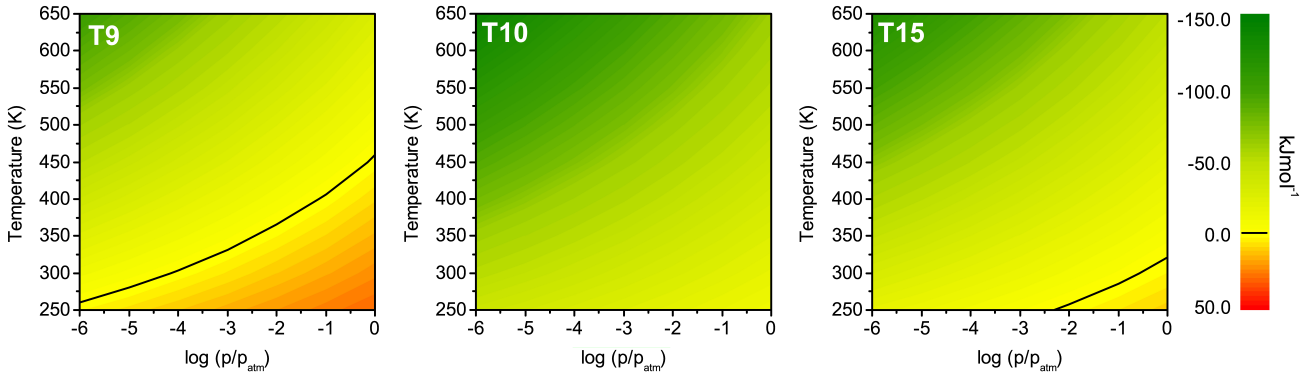


Figure 4. ΔG (for the second $NH_3$ molecule desorption process) *vs.* temperature and pressure (expressed as logarithm of the ratio with $p_{atm}$) behaviors computed for the three most stable T sites: T9, T10 and T15. The solid black contour line shows the $\Delta G = 0$ kJ $mol^{-1}$ threshold, *i.e.* where desorption turns favorable ($\Delta G < 0$) further increasing the temperature or reducing the pressure.

Excluding the photochemical phenomena which occur, this energy is most probably converted to heat:[70] if the sample temperature rises during the experiment, the weakest interacting adsorbates could be desorbed. Furthermore, the previous experiments were carried out at a pressure lower than atmospheric (hereafter $p_{atm}$ = 101325 Pa), *i.e.* decreasing the stability of the Ti–$NH_3$ adducts. Thereby, the ΔG relation with temperature and pressure was considered. In detail, the Gibbs free energy for desorption of the second $NH_3$ molecule (*i.e.* inverting the process depicted in Equation 5) was computed as a function of temperature and pressure for the three sites. The obtained trends are reported in Figure 4. The same observation previously based on the STP energetic only are confirmed by this new dataset. T9 is definitely able to host two $NH_3$ molecules in a wide range of temperatures and pressures: at $p_{atm}$ the desorption of the second ammonia favored only above ~450 K, whereas at RT occurs just at very low pressures ($p < 10^{-4}$ Pa). This suggests the double $NH_3$ adduct should survive to the measurement conditions experienced under a synchrotron radiation beam. T10 instead presents a situation strongly unfavorable to a second adsorption: even at temperature significantly lower than RT, the desorption ΔG for the second $NH_3$ molecule sticks to negative values. Furthermore, extrapolating from the trend the temperature where ΔG is nil, a value of ~170 K, lower than the condensation temperature of gaseous ammonia (240 K),[71] is obtained. The same stands for pressure, as at RT (even at values close to $p_{atm}$) the second adsorption is not favored. Finally, T15 shows as the desorption of the second $NH_3$ molecules turns probable at easily accessible temperature values, with its related desorption ΔG turning negative at a temperature of ~320 K at $p_{atm}$ or at a pressure $< 10^{-1}$ Pa at RT. The latter case, the Ti-$(NH_3)$ $\rightleftharpoons$ Ti-$(NH_3)_2$ equilibrium could be displaced to the left-hand side by beam induced heating, especially when the data collection (vtc-XES) required the use of high photon flux undulators (three orders of magnitude more brilliant than bending magnets used in most of the EXAFS beamlines) and long exposure times. Apart from the determination of the bare adsorptive properties, the simulation of TS-1 adducts with basic molecules could have a role in the correct determination of the relative stabilities of the various T sites. As already documented by Ricchiardi et al.,[28] the presence of these bases coordinated to Ti (in the specific case, water molecules) affects the stability ranking computed in their absence. The capability to coordinate bases (which are ubiquitous in the synthetic environment of TS-1)[1] with a consistent energy gain (*e.g.* see Table 2) is thus a relevant parameter in the preferable insertion of Ti in a specific T site. Considering the absolute energies upon double ammonia adsorption, the site ranking switches from T10 < T9 < T15 to T9 < T15 < T10. The energy splitting among the sites sensibly increases too, with T9 being now 16.3 $kJmol^{-1}$ and 29.0 $kJmol^{-1}$ more sta-

ble than T15 and T10 respectively. Furthermore, considering that T10 is reasonably able to host a single $NH_3$ molecule only, its energetic spread from T9 further raises to 80.9 $kJmol^{-1}$, a value suggesting its probable exclusion from the list of the most populated sites. Such results suggest as (in a barely thermodynamic framework) keeping in account the presence of basic molecules in the synthesis environment of TS-1 may significantly affect the Ti distribution among the sites. Surely this type of behavior requires further investigation, taking into account the totality of the independent T sites.

## 4. CONCLUSIONS

The present study reported for the first time an accurate simulation of TS-1 with low Ti content (Si/Ti = 95) with a periodic, all-electron B3LYP-D2 approach. The monoclinic structure of MFI, experimentally recognized to occur at low Ti loadings, was exploited in the calculations: all the 24 independent T sites were considered and ranked on the basis of their relative energies. The geometrical description of the system, considered in an averaged way, has a reasonable qualitative agreement with the experimental data. Concerning adsorption properties, the key role of the local environment surrounding the Ti site has been highlighted. On the contrary, the relative stability of the Ti sites does not significantly affect the adsorption strength. In particular, each of the five considered T sites is able to form stable $NH_3$ mono-adducts. Conversely, the adsorption of a second $NH_3$ molecule is strongly site dependent. T9 fully allows the coordination of a second $NH_3$ molecule, with a stability similar to the first one. Remarkably, T4 and T10 prefer a five-coordination, as the adsorption of a second $NH_3$ molecule is very unlikely to occur (even at temperatures lower than RT and pressures close to $p_{atm}$) according to the estimated $\Delta G$. Moreover, T15 and T24 have an intermediate behavior and they are able to coordinate two $NH_3$ molecules, but only when the temperature is lower than RT and the pressure is not significantly lower than $p_{atm}$. Finally, the different adsorption capability (in terms of stability of the TS-1–$NH_3$ adducts) of the considered T sites points to reconsider the relative stability ranking, since the presence of adsorbed basic molecules could affect the Ti insertion in a thermodynamic regime.

## ASSOCIATED CONTENT

### Supporting Information

Relative stabilities of Ti sites placed in the 24 T sites of MFI, numerical values (Table S1); Si → Ti Substitution energies for the 24 T sites (Figure S1); Si → Ti Substitution energies for the 24 T sites, numerical values (Table S2); full set of geometrical parameters for the TS-1 structures (Table S3); structural data for $E_{min}$ models, *TS1_calc_SI.pdf*

Animated structure of T9 site, *t9.avi*

Animated structure of T10 site, *t10.avi*

Animated structure of T15 site, *t15.avi*

The Supporting Information is available free of charge on the ACS Publications website.

## AUTHOR INFORMATION


### Corresponding Author

* Alessandro Damin, Tel: +39-011-6708383, Fax: +39-011-6707855, E-mail: alessandro.damin@unito.it


## ACKNOWLEDGMENT


The authors acknowledge CINECA and NOTUR consortia, granting computational time on the Marconi and Abel clusters respectively through the projects ISCRA-C "MoTiZ" and N9381K. The authors acknowledge the theoretical chemistry group (Department of Chemistry, Università di Torino) for providing the CRYSTAL14 code. C.L. acknowledges the Mega-Grant from the Ministry of Education and Science of the Russian Federation (14.Y26.31.0001). The authors acknowledge Evonik Industries AG for the support to this research.


## REFERENCES


(1) Notari, B.; Perego, G.; Taramasso, M. Preparation of Porous Crystalline Synthetic Material Comprised of Silicon and Titanium Oxides. US4410501 A, 1983.

(2) Xu, L.; Ding, J.; Yang, Y.; Wu, P. Distinctions of Hydroxylamine Formation and Decomposition in Cyclohexanone Ammoximation over Microporous Titanosilicates. *J. Catal.* **2014**, *309*, 1–10.

(3) Zecchina, a.; Bordiga, S.; Lamberti, C.; Ricchiardi, G.; Lamberti, C.; Ricchiardi, G.; Scarano, D.; Petrini, G.; Leofanti, G.; Mantegazza, M. Structural Characterization of Ti Centres in Ti-Silicalite and Reaction Mechanisms in Cyclohexanone Ammoximation. *Catal. Today* **1996**, *32* (1–4), 97–106.

(4) Roffia, P.; Leofanti, G.; Cesana, A.; Mantegazza, M.; Padovan, M.; Petrini, G.; Tonti, S.; Gervasutti, P. Cyclohexanone Ammoximation: A Break Through In The 6-Caprolactam Production Process. In *Studies in Surface Science and Catalysis*; Centi, G., Trifiro F., Eds.; **1990**; Vol. *55*, pp 43–52.

(5) Roffia, P.; Padovan, M.; Moretti, E.; De Alberti, G. Catalytic Process for Preparing Cyclohexanone-Oxime. US 4745221 (A), May 17, 1988.

(6) Bregante, D. T.; Flaherty, D. W. Periodic Trends in Olefin Epoxidation over Group IV and v Framework-Substituted Zeolite Catalysts: A Kinetic and Spectroscopic Study. *J. Am. Chem. Soc.* **2017**, *139* (20), 6888–6898.

(7) Notari, B. Microporous Crystalline Titanium Silicates. In *Advances in Catalysis*; Eley, D. D., Haag, W. O., Gates, B., Eds.; Elsevier Academic Press Inc: San Diego, **1996**; *Vol. 41*, pp 253–334.

(8) Romano, U.; Ricci, M. Industrial Applications. In *Liquid Phase Oxidation via Heterogeneous Catalysis*; Clerici, M. G., Kholdeeva, O. A., Eds.; John Wiley & Sons, Inc.: Hoboken, New Jersey, **2013**; pp 451–506.

(9) Schmidt, F.; Bernhard, M.; Morell, H.; Pascaly, M. HPPO Process Technology A Novel Route to Propylene Oxide without Coproducts. *Chem. Today* **2014**, *32* (2), 31–35.

(10) Millini, R.; Massara, E. P.; Perego, G.; Bellussi, G.; Previde Massara, E.; Perego, G.; Bellussi, G. Framework Composition of Titanium Silicalite-1. *J. Catal.* **1992**, *137* (2), 497–503.

(11) Lamberti, C.; Bordiga, S.; Zecchina, A.; Carati, A.; Fitch, N. N.; Artioli, G.; Petrini, G.; Salvalaggio, M.; Marra, G. L. L. Structural Characterization of Ti-Silicalite-1: A Synchrotron Radiation X-Ray Powder Diffraction Study. *J. Catal.* **1999**, *183* (2), 222–231.

(12) Lamberti, C.; Bordiga, S.; Zecchina, A.; Artioli, G.; Marra, G.; Spanò, G. Ti Location in the MFI Framework of Ti-Silicalite-1: A Neutron Powder Diffraction Study. *J. Am. Chem. Soc.* **2001**, *123* (10), 2204–2212.

(13) Bordiga, S.; Damin, A.; Bonino, F.; Ricchiardi, G.; Lamberti, C.; Zecchina, A. The Structure of the Peroxo Species in the TS-1 Catalyst as Investigated by Resonant Raman Spectroscopy. *Angew. Chem. Int. Ed.* **2002**, *41* (24), 4734–4737.

(14) Li, C.; Xiong, G.; Liu, J.; Ying, P.; Xin, Q.; Feng, Z. Identifying Framework Titanium in TS-1 Zeolite by UV Resonance Raman Spectroscopy. *J. Phys. Chem. B* **2001**, *105* (15), 2993–2997.

(15) Bordiga, S.; Damin, A.; Bonino, F.; Ricchiardi, G.; Zecchina, A.; Tagliapietra, R.; Lamberti, C. Resonance Raman Effects in TS-1: The Structure of Ti(iv) Species and Reactivity towards $H_2O$, $NH_3$ and $H_2O_2$: An in Situ study. *Phys. Chem. Chem. Phys.* **2003**, *5* (20), 4390–4393.

(16) Fan, F.; Feng, Z.; Li, C. UV Raman Spectroscopic Studies on Active Sites and Synthesis Mechanisms of Transition Metal-Containing Microporous and Mesoporous Materials. *Acc. Chem. Res.* **2010**, *43* (3), 378–387.

(17) Guo, Q.; Feng, Z.; Li, G.; Fan, F.; Li, C. Finding the "Missing Components" during the Synthesis of TS-1 Zeolite by UV Resonance Raman Spectroscopy. *J. Phys. Chem. C* **2013**, *117* (6), 2844–2848.

(18) Zuo, Y.; Liu, M.; Zhang, T.; Hong, L.; Guo, X.; Song, C.; Chen, Y.; Zhu, P.; Jaye, C.; Fischer, D. Role of Pentahedrally Coordinated Titanium in Titanium Silicalite-1 in Propene Epoxidation. *Rsc Adv.* **2015**, *5* (23), 17897–17904.

(19) Bordiga, S.; Coluccia, S.; Lamberti, C.; Marchese, L.; Zecchina, A.; Boscherini, F.; Buffa, F.; Genoni, F.; Leofanti, G.; Coluccia, S.; et al. XAFS Study of Ti-Silicalite: Structure of Framework Ti(IV) in the Presence and Absence of Reactive Molecules ($H_2O$, $NH_3$) and Comparison with Ultraviolet-Visible and IR Results. *J. Phys. Chem.* **1994**, *98* (15), 4125–4132.

(20) Gleeson, D.; Sankar, G.; Richard A. Catlow, C.; Meurig Thomas, J.; Spanó, G.; Bordiga, S.; Zecchina, A.; Lamberti, C. The Architecture of Catalytically Active Centers in Titanosilicate (TS-1) and Related Selective-Oxidation Catalysts. *Phys. Chem. Chem. Phys.* **2000**, *2* (20), 4812–4817.

(21) Zecchina, A.; Bordiga, S.; Spoto, G.; Damin, A.; Berlier, G.; Bonino, F.; Prestipino, C.; Lamberti, C. In Situ Characterization of Catalysts Active in Partial Oxidations: TS-1 and Fe-MFI Case Studies. *Top. Catal.* **2002**, *21* (1–3), 67–78.

(22) Milanesio, M.; Artioli, G.; Gualtieri, A. F.; Palin, L.; Lamberti, C. Template Burning inside TS-1 and Fe-MFI Molecular Sieves: An in Situ XRPD Study. *J. Am. Chem. Soc.* **2003**, *125* (47), 14549–14558.

(23) Bonino, F.; Damin, A.; Ricchiardi, G.; Ricci, M.; Spanò, G.; D'Aloisio, R.; Zecchina, A.; Lamberti, C.; Prestipino, C.; Bordiga, S. Ti-Peroxo Species in the TS-1/$H_2O_2$/$H_2O$ System. *J. Phys. Chem. B* **2004**, *108* (11), 3573–3583.

(24) Ricchiardi, G.; Damin, A.; Bordiga, S.; Lamberti, C.; Spano, G.; Rivetti, F.; Zecchina, A.; Spanò, G.; Rivetti, F.; Zecchina, A. Vibrational Structure of Titanium Silicate Catalysts. A Spectroscopic and Theoretical Study. *J. Am. Chem. Soc.* **2001**, *123* (46), 11409–11419.

(25) Li, C.; Xiong, G.; Xin, Q.; Liu, J. K.; Ying, P. L.; Feng, Z. C.; Li, J.; Yang, W. Bin; Wang, Y. Z.; Wang, G. R.; et al. UV Resonance Raman Spectroscopic Identification of Titanium Atoms in the Framework of TS-1 Zeolite. *Angew. Chem. Int. Ed.* **1999**, *38* (15), 2220–2222.

(26) Fan, F.; Feng, Z.; Li, C. UV Raman Spectroscopic Study on the Synthesis Mechanism and Assembly of Molecular Sieves. *Chem. Soc. Rev.* **2010**, *39* (12), 4794–4801.

(27) Bordiga, S.; Boscherini, F.; Coluccia, S.; Genonic, F.; Lamberti, C.; Leofanti, G.; Marchese, L.; Petrini, G.; Vlaic, G.; Zecchina, A. XAFS Study of Ti-Silicalite: Structure of Framework Ti(IV) in Presence and in Absence of Reactive Molecules ($H_2O$, $NH_3$). *Catal. Letters* **1994**, *26* (1–2), 195–208.

(28) Ricchiardi, G.; de Man, A.; Sauer, J. The Effect of Hydration on Structure and Location of Ti-Sites in Ti-Silicalite Catalysts. A Computational Study. *Phys. Chem. Chem. Phys.* **2000**, *2* (10), 2195–2204.

(29) Damin, A.; Bordiga, S.; Zecchina, A.; Lamberti, C. Reactivity of Ti(IV) Sites in Ti-Zeolites: An Embedded Cluster Approach. *J. Chem. Phys.* **2002**, *117* (1), 226–237.

(30) Gale, J. D. A Periodic Density Functional Study of the Location of Titanium within TS-1. *Solid State Sci.* **2006**, *8* (3–4 SPEC. ISS.), 234–240.

(31) Fois, E.; Gamba, A.; Tabacchi, G. Bathochromic Effects in Electronic Excitation Spectra of Hydrated Ti Zeolites: A Theoretical Characterization. *ChemPhysChem* **2008**, *9* (4), 538–543.

(32) Gamba, A.; Tabacchi, G.; Fois, E. TS-1 from First Principles. *J. Phys. Chem. A* **2009**, *113* (52), 15006–15015.

(33) Dong, J.; Zhu, H.; Xiang, Y.; Wang, Y.; An, P.; Gong, Y.; Liang, Y.; Qiu, L.; Zheng, A.; Peng, X.; et al. Toward a Unified Identification of Ti Location in the MFI Framework of High-Ti-Loaded TS-1: Combined EXAFS, XANES, and DFT Study. *J. Phys. Chem. C* **2016**, *120* (36), 20114–20124.

(34) Damin, A.; Bordiga, S.; Zecchina, A.; Doll, K.; Lamberti, C. Ti-Chabazite as a Model System of Ti(IV) in Ti-Zeolites: A Periodic Approach. *J. Chem. Phys.* **2003**, *118* (22), 10183–10194.

(35) Gallo, E.; Lamberti, C.; Glatzel, P. Investigation of the Valence Electronic States of Ti(iv) in Ti Silicalite-1 Coupling X-Ray Emission Spectroscopy and Density Functional Calculations. *Phys. Chem. Chem. Phys.* **2011**, *13* (43), 19409.

(36) Al Derzi, A. R.; Gregušová, A.; Runge, K.; Bartlett, R. J. Structure and Properties of Disiloxane: An Ab Initio and Post-Hartree-Fock Study. *Int. J. Quantum Chem.* **2008**, *108* (12), 2088–2096.

(37) Csonka, G. I. The Failure of the MO-Based Theoretical Disiloxane Explanations. *J. Mol. Struct.* **1995**, *332*, 187–188.

(38) Csonka, G. I.; Réffy, J. Density Functional Study of the Equilibrium Geometry and Si-O-Si Potential Energy Curve of Disiloxane. *Chem. Phys. Lett.* **1994**, *229* (3), 191–197.

(39) Cypryk, M.; Gostyński, B. Computational Benchmark for Calculation of Silane and Siloxane Thermochemistry. *J. Mol. Model.* **2016**, *22* (1), 1–19.

(40) Zicovich-Wilson, C. M.; Dovesi, R. Titanium-Containing Zeolites. A Periodic Ab Initio Hartree Fock Characterization. *J. Phys. Chem. B* **1998**, *102* (8), 1411–1417.

(41) Zicovich-Wilson, C. M.; Dovesi, R.; Corma, A. Interaction of Ti-Zeolites with Water. A Periodic Ab Initio Study. *J. Phys. Chem. B* **1999**, *103* (6), 988–994.

(42) Signorile, M.; Damin, A.; Bonino, F.; Crocellà, V.; Lamberti, C.; Bordiga, S. The Role of Dispersive Forces Determining the Energetics of Adsorption in Ti Zeolites. *J. Comput. Chem.* **2016**, *37* (30), 2659–2666.

(43) Eilertsen, E. A.; Bordiga, S.; Lamberti, C.; Damin, A.; Bonino, F.; Arstad, B.; Svelle, S.; Olsbye, U.; Lillerud, K. P. Synthesis of Titanium Chabazite: A New Shape Selective Oxidation Catalyst with Small Pore Openings and Application in the Production of Methyl Formate from Methanol. *ChemCatChem* **2011**, *3* (12), 1869–1871.

(44) Bolis, V.; Bordiga, S.; Lamberti, C.; Zecchina, A.; Carati, A.; Rivetti, F.; Spanò, G.; Petrini, G. Heterogeneity of Framework Ti(IV) in Ti−Silicalite as Revealed by the Adsorption of $NH_3$. Combined Calorimetric and Spectroscopic Study. *Langmuir* **1999**, *15* (18), 5753–5764.

(45) Bolis, V.; Bordiga, S.; Lamberti, C.; Zecchina, A.; Carati, A.; Rivetti, F.; Petrini, G.; Spanò, G. A Calorimetric , IR , XANES and EXAFS Study

of the Adsorption of NH on Ti-Silicalite as a Function of the Sample Pre-Treatment. *Microporous Mesoporous Mater.* **1999**, *30*, 67–76.
(46) Gallo, E.; Bonino, F.; Swarbrick, J. C.; Petrenko, T.; Piovano, A.; Bordiga, S.; Gianolio, D.; Groppo, E.; Neese, F.; Lamberti, C.; et al. Preference towards Five-Coordination in Ti Silicalite-1 upon Molecular Adsorption. *ChemPhysChem* **2013**, *14* (1), 79–83.
(47) Marra, G. L.; Artioli, G.; Fitch, A. N.; Milanesio, M.; Lamberti, C. Orthorhombic to Monoclinic Phase Transition in High-Ti-Loaded TS-1: An Attempt to Locate Ti in the MFI Framework by Low Temperature XRD. *Microporous Mesoporous Mater.* **2000**, *40* (1–3), 85–94.
(48) Artioli, G.; Lamberti, C.; Marra, G. L. Neutron Powder Diffraction Study of Orthorhombic and Monoclinic Defective Silicalite. *Acta Crystallogr. Sect. B Struct. Sci.* **2000**, *56* (1), 2–10.
(49) Dovesi, R.; Orlando, R.; Erba, A.; Zicovich-Wilson, C. M.; Civalleri, B.; Casassa, S.; Maschio, L.; Ferrabone, M.; De La Pierre, M.; D'Arco, P.; et al. CRYSTAL14 : A Program for the *Ab Initio* Investigation of Crystalline Solids. *Int. J. Quantum Chem.* **2014**, *114* (19), 1287–1317.
(50) Becke, A. D. A New Mixing of Hartree–Fock and Local Density-functional Theories. *J. Chem. Phys.* **1993**, *98* (2), 1372–1377.
(51) Lee, C.; Yang, W.; Parr, R. G. Development of the Colle-Salvetti Correlation-Energy Formula into a Functional of the Electron Density. *Phys. Rev. B* **1988**, *37* (2), 785–789.
(52) Grimme, S. Semiempirical GGA-Type Density Functional Constructed with a Long-Range Dispersion Correction. *J. Comput. Chem.* **2006**, *27* (15), 1787–1799.
(53) Gale, J. D. GULP: A Computer Program for the Symmetry-Adapted Simulation of Solids. *J. Chem. Soc. Faraday Trans.* **1997**, *93* (4), 629–637.
(54) Sierka, M.; Joachim Sauer, A. Structure and Reactivity of Silica and Zeolite Catalysts by a Combined Quantum Mechanics Shell-Model Potential Approach Based on DFT. *Faraday Discuss.* **1997**, *106*, 41–62.
(55) Available at: http://www.crystal.unito.it/Basis_Sets/titanium.html#Ti_86-411%28d31%29G_darco_unpub.
(56) Nada, R.; Nicholas, J. B.; McCarthy, M. I.; Hess, A. C. Basis Sets for Ab Initio Periodic Hartree-Fock Studies of Zeolite/adsorbate Interactions: He, Ne, and Ar in Silica Sodalite. *Int. J. Quantum Chem.* **1996**, *60*, 809–820.
(57) Schäfer, A.; Huber, C.; Ahlrichs, R. Fully Optimized Contracted Gaussian Basis Sets of Triple Zeta Valence Quality for Atoms Li to Kr. *J. Chem. Phys.* **1994**, *100* (8), 5829–5835.
(58) Dovesi R.; Saunders, V. R.; Roetti, C.; Orlando, R.; Zicovich-Wilson, C. M.; Pascale, F.; Civalleri, B.; Doll, K.; Harrison, N. M.; Bush, I. J.; et al. CRYSTAL14 User's Manual. *http://www.crystal.unito.it/Manuals/crystal14.pdf* **2014**.
(59) Piccini, G.; Alessio, M.; Sauer, J.; Zhi, Y.; Liu, Y.; Kolvenbach, R.; Jentys, A.; Lercher, J. A. Accurate Adsorption Thermodynamics of Small Alkanes in Zeolites. Ab Initio Theory and Experiment for H-Chabazite. *J. Phys. Chem. C* **2015**, *119* (11), 6128–6137.
(60) Henry, P. F.; Weller, M. T.; Wilson, C. C. Structural Investigation of TS-1: Determination of the True Nonrandom Titanium Framework Substitution and Silicon Vacancy Distribution from Powder Neutron Diffraction Studies Using Isotopes. *J. Phys. Chem. B* **2001**, *105* (31), 7452–7458.
(61) Hijar, C. A.; Jacubinas, R. M.; Eckert, J.; Henson, N. J.; Hay, P. J.; Ott, K. C. The Siting of Ti in TS-1 Is Non-Random. Powder Neutron Diffraction Studies and Theoretical Calculations of TS-1 and FeS-1. *J. Phys. Chem. B* **2000**, *104* (51), 12157–12164.
(62) Atoguchi, T.; Yao, S. Ti Atom in MFI Zeolite Framework: A Large Cluster Model Study by ONIOM Method. *J. Mol. Catal. A Chem.* **2003**, *191* (2), 281–288.
(63) Deka, R. C.; Nasluzov, V. A.; Ivanova Shor, E. A.; Shor, A. M.; Vayssilov, G. N.; Rösch, N. Comparison of All Sites for Ti Substitution in Zeolite TS-1 by an Accurate Embedded-Cluster Method. *J. Phys. Chem. B* **2005**, *109* (51), 24304–24310.
(64) Yuan, S.; Si, H.; Fu, A.; Chu, T.; Tian, F.; Duan, Y. B.; Wang, J. Location of Si Vacancies and [Ti(OSi)4] and [Ti(OSi) 3OH] Sites in the MFI Framework: A Large Cluster and Full Ab Initio Study. *J. Phys. Chem. A* **2011**, *115* (5), 940–947.
(65) Montejo-Valencia, B. D.; Salcedo-Pérez, J. L.; Curet-Arana, M. C. DFT Study of Closed and Open Sites of BEA, FAU, MFI, and BEC Zeolites Substituted with Tin and Titanium. *J. Phys. Chem. C* **2016**, *120* (4), 2176–2186.
(66) Lamberti, C.; Bordiga, S.; Arduino, D.; Zecchina, A.; Geobaldo, F.; Spano, G.; Genoni, F.; Petrini, G.; Carati, A.; Villain, F.; et al. Evidence of the Presence of Two Different Framework Ti(IV) Species in Ti−Silicalite-1 in Vacuo Conditions: An EXAFS and a Photoluminescence Study. *J. Phys. Chem. B* **1998**, *102* (33), 6382–6390.
(67) Bordiga, S.; Roggero, I.; Ugliengo, P.; Zecchina, A.; Bolis, V.; Artioli, G.; Buzzoni, R.; Marra, G.; Rivetti, F.; Spanò, G.; et al. Characterisation of Defective Silicalites. *J. Chem. Soc. Dalt. Trans.* **2000**, *21*, 3921–3929.
(68) Bordiga, S.; Ugliengo, P.; Damin, A.; Lamberti, C.; Spoto, G.; Zecchina, A.; Spano, G.; Buzzoni, R.; Dalloro, L.; Rivetti, F. Hydroxyls Nests in Defective Silicalites and Strained Structures Derived upon Dehydroxylation: Vibrational Properties and Theoretical Modelling. *Top. Catal.* **2001**, *15* (1), 43–52.
(69) Marra, G. L.; Tozzola, G.; Leofanti, G.; Padovan, M.; Petrini, G.; Genoni, F.; Venturelli, B.; Zecchina, A.; Bordiga, S.; Ricchiardi, G. Orthorhombic and Monoclinic Silicalites: Structure, Morphology, Vibrational Properties and Crystal Defects. In *Studies in Surface Science and Catalysis*; Weitkamp, J., Karge, H.G., Pfeifer, H., Hölderich, W., Eds.; **1994**; *Vol. 84*, pp 559–566.
(70) Snell, E. H.; Bellamy, H. D.; Rosenbaum, G.; Van Der Woerd, M. J. Non-Invasive Measurement of X-Ray Beam Heating on a Surrogate Crystal Sample. *J. Synchrotron Radiat.* **2007**, *14* (1), 109–115.
(71) Haynes, W. M. *CRC Handbook of Chemistry and Physics 97th Edition*; 2017.

**TOC Graphic**